J Solid State Electrochem (1998) 2: 420–426

ORIGINAL PAPER

J. Morales · L. Sánchez · J.L. Tirado

New doped Li-M-Mn-O (M = Al, Fe, Ni) spinels as cathodes for rechargeable 3 V lithium batteries

Received: 25 November 1997 / Accepted: 28 January 1998

Abstract The electrochemical behaviour of new doped Li-M-Mn-O (M = Al, Fe, Ni) spinel oxides in liquid electrolyte lithium cells was studied. The insertion electrode materials were obtained by heating stoichiometric amounts of thoroughly mixed LiOH and $M_xMn_{1-x}CO_3$ (M = Fe, Ni; $x = 0.08-0.15$) or $Al_xMn_{1-x}(CO_3)(OH)_y$, in the case of Al, at 380 °C in air for 20 h. The transition metal-doped samples, particularly those containing Ni or obtained at low temperatures, where the resulting spinel was cation-deficient and highly disordered, exhibited the best cycling performance in the potential window 3.3–2.3 V. Cell capacity was retained by 80% after 200 cycles. Capacity fading was observed on increasing the firing temperature, together with improved crystallinity and the disappearance of cation vacancies. This impaired electrochemical behaviour is ascribed to a Jahn-Teller effect, which induces an X-ray-detectable cubic-tetragonal phase transition upon lithium insertion. The phase transition was undetectable in the low-temperature samples. The influence of the Jahn-Teller distortion is thus seemingly lessened by a highly disordered structure.

Key words Doped manganese spinels · Lithium, lithium battery · Electrochemical intercalation reaction

Introduction

The spinel $LiMn_2O_4$ has been extensively studied on account of its potential as a commercial cathode material for secondary lithium batteries [1–6]. This material, which is more affordable and less toxic than other transition metal oxides, has the ability to incorporate a second lithium atom at 3 V, leading to the formation of a tetragonal $Li_2Mn_2O_4$ phase. The concurrent cubic to tetragonal phase change is believed to detract from the electrochemical performance of this material [6]. The capacity loss on cycling at 3 V is thought to be mainly a result of Jahn-Teller distortion, which causes a 16% increase in the c/a ratio of the unit cell during extraction of lithium and insertion into $LiMn_2O_4$ electrodes [6]. Such an increase is too large for the electrode to maintain its structural integrity on cycling. Therefore, this material has limited use in rechargeable 3-V lithium cells.

Several methods have been proposed to overcome the above-mentioned Jahn-Teller distortion effect. These involve altering the synthetic conditions [4, 7], using metal-substituted spinels [8] or employing alternative stoichiometric and defective spinel phases [9]. Also, some properties of the active material – usually prepared via solid-state reactions – such as grain size, oxygen content, number of vacancies, etc., have been shown to play a major role in its electrochemical behaviour.

On the other hand, excellent capacity retention on cycling has been obtained from Li-Mn-O cathodes in the Li_2O-$y$$MnO_2$ system. Particularly good in this respect are $Li/Li_2Mn_4O_9$ ($y = 4$) and $Li/Li_4Mn_5O_{12}$ ($y = 2.5$) cells [6] when cycled over the range 2.3–3.3 V. These systems possess several attractive features, namely: (1) the compounds can be easily prepared in a few hours below 400 °C, (2) the resulting cells exhibit high theoretical capacities (viz. 213 Ah/kg and 163 Ah/kg for $Li_2Mn_4O_9$ and $Li_4Mn_5O_{12}$, respectively), and (3) Li/Li_2O-$y$$MnO_2$ cells are more stable on cycling than are $Li/Li[Mn_2]O_4$ cells. This superior cycling behaviour has been attributed to the fact that lithium is inserted into cubic Li_2O-$y$$MnO_2$ spinel structures with minimal increase in unit-cell volume and that the Jahn-Teller effect occurs late in the discharge reaction, when the average valence of the manganese ions is about 3.5. However, no experimental extended cycling data for the Li_2O-$y$$MnO_2$ have so far been reported.

J. Morales · L. Sánchez (✉) · J.L. Tirado
Laboratorio de Química Inorgánica, Facultad de Ciencias, Universidad de Córdoba, Avda. S. Alberto Magno s/n, E-14004 Córdoba, Spain

We have developed an alternative method for improving the electrochemical performance of the $LiMn_2O_4$ spinel as a cathode in 3-V lithium cells by replacing Mn partially with Co [10]. This spinel was prepared via a solution technique to obtain an ultrafine carbonate precursor of composition $Co_{0.14}Mn_{0.86}CO_3$. The presence of cobalt was essential to avoid the structural distortion caused by the Jahn-Teller effect. Especially good performance was obtained from $Li/Li_{2.13}Co_{0.57}Mn_{3.66}O_4$ cells cycled between 3.3 and 2.3 V. These cells exhibit better cycling properties than those of $Li/Li_{1+x}Mn_{2-x}O_4$ and Li/Li_2O-$yMnO_2$ ($y = 4, 2.5$).

The promising features of the Co system prompted us to extend these studies to other dopant metals such as Al, Fe and Ni, which are quite abundant and less expensive and contaminant. This paper reports on the preparation and characterization of these 3-V spinels, in addition to a detailed study of the battery characterization and performance.

Experimental

Mixed manganese dopant-metal precursors were prepared by adding a 1 M solution of $NaHCO_3$ to a 0.5 M solution of the divalent ions Mn(II) and M(II) [M = Fe, Ni] (using a trivalent salt for Al) under a continuous flow of CO_2. The Li-M-Mn-O spinel phases were synthesized by heating stoichiometric amounts of thoroughly mixed LiOH and the precursors (obtained under the above experimental conditions) at 380°C in air for 20 h. The respective precursors were prepared in an M/Mn ratio of 0.17. However, this ratio was only obtained for the Fe-Mn precursor. The Ni-Mn and Al-Mn precursors exhibited an M/Mn ratio of 0.09. A more alkaline pH was required probably to prepare the carbonate precursor in order to ensure effective doping. This differential M/Mn ratio is reflected in the spinel oxide composition shown in Table 1. Stoichiometries were confirmed by atomic absorption spectrometry (AAS), inductively coupled plasma (ICP) and electron microprobe energy dispersive X-ray analysis (EDXA).

The average oxidation state of Mn ion was determined by the following procedure. About 20 mg of sample was dissolved in 40 ml of 0.1 M Fe^{2+} in 0.01 M H_2SO_4 under a continuous flow of argon, with heating until complete dissolution was achieved. The solution was titrated with standard 0.01 $KMnO_4$. Previously, the $KMnO_4$ solution was standardized with $Na_2C_2O_4$. Titrant consumption was assigned to excess of Fe^{2+} ions in the sample solution and used to calculate the oxygen-to-metal ratios.

XRD patterns were recorded on a Siemens D-5000 X-ray diffractometer, using CuKα radiation and graphite monochromator. Scanning electron micrographs were obtained on a JEOL JSM6300 microscope.

Electrochemical experiments were carried out in two-electrode cells, using lithium as anode. The electrolyte used was 1 M $LiClO_4$, previously dried at 170°C in vacuo for 16 h, in 1:1 distilled ethylene/propylene carbonate. Oxide electrode pellets (7 mm diameter) were prepared by pressing ca. 3 mg of active material with polytetrafluoroethylene (PTFE) [5 weight percent (w/o)], graphite (7.5 w/o) and acetylene black (7.5 w/o) at 4 tons. Lithium foil was cut as circles of 7 mm diameter and used as anodes against each spinel oxide electrode. Unless otherwise specified, cells were cycled at a 0.25 mA/cm^2 current density and controlled via a MacPile II potentiostat-galvanostat. Step potential electrochemical spectroscopy (SPES) spectra were recorded in 1.25-mV steps of 30 s duration.

Results and discussion

Figure 1 shows the XRD patterns for the oxides obtained by thermal decomposition of a mixture of LiOH and the different mixed carbonate $M_xMn_{1-x}CO_3$ (M = Fe, Ni) precursors in the air at 380°C for 20 h.

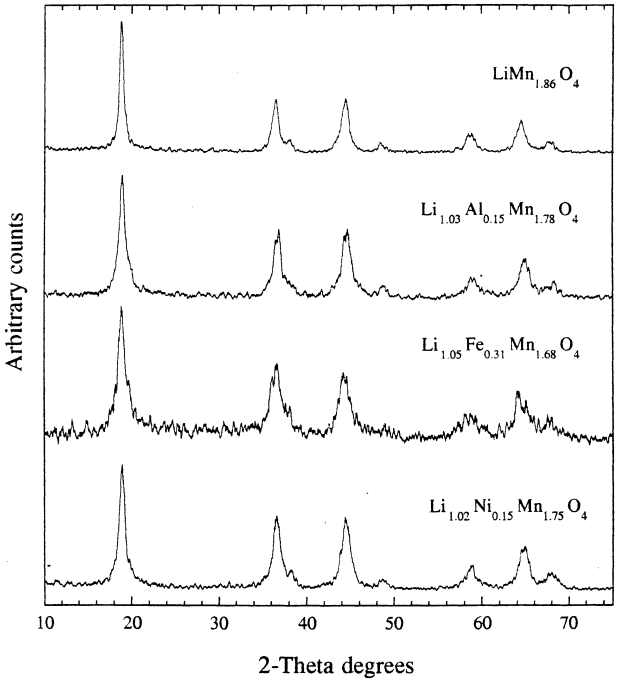

Fig. 1 Powder X-ray diffraction patterns for the products obtained in the thermal decomposition of a mixture of LiOH and various mixed carbonates in the air at 380 °C for 20 h

Table 1 Chemical and crystallographic data for Li-M-Mn-O spinels

Composition	T (°C)	a (Å)	O/(Li + M + Mn)	Q^a_{theor}	(M + Mn)/Li	Z_{Mn}
$LiMn_{1.86}O_4$	380	8.166 (2)	1.40	176.5	1.86	3.76
$Li_{1.03}Al_{0.15}Mn_{1.78}O_4$	380	8.110 (1)	1.38	172.3	1.87	3.66
$Li_{1.05}Fe_{0.31}Mn_{1.68}O_4$	380	8.12 (1)	1.32	142.2	1.89	3.54
$Li_{1.02}Ni_{0.15}Mn_{1.75}O_4$	380	8.149 (4)	1.37	164.5	1.86	3.81
$Li_{1.02}Ni_{0.15}Mn_{1.75}O_{3.88}$	550	8.177 (2)	1.33	148.7	1.86	3.68
$Li_{1.02}Ni_{0.15}Mn_{1.75}O_{3.82}$	800	8.197 (3)	1.31	138.9	1.86	3.61

[a] Theoretical capacity (Ah/kg) to reach a rock-salt stoichiometry

The Al precursor can be tentatively formulated as a hydroxycarbonate of the type $Al_xMn_{1-x}(CO_3)(OH)_x$. The different spectra can be indexed according to a single phase with a cubic spinel structure. On the other hand, the XRD patterns exhibit broad peaks, as is usually the case with solids obtained by low-temperature thermal decomposition of precursor compounds, and this makes it difficult to observe the presence of other potential manganese phases ($Li_2Mn_4O_9$, $Li_4Mn_5O_{12}$, Li_2MnO_3, $LiMnO_2$). Table 1 summarizes the chemical and crystallographic properties of these Li-M-Mn-O spinel oxides.

Based on metal content, two types of spinel were prepared, namely: cation-deficient for the $LiMn_{1.86}O_4$, $Li_{1.02}Ni_{0.15}Mn_{1.75}O_4$ and $Li_{1.03}Al_{0.15}Mn_{1.78}O_4$ systems, and oxygen-deficient for the $Li_{1.05}Fe_{0.31}Mn_{1.68}O_4$ system. The $LiMn_{1.86}O_4$ and $Li_{1.02}Ni_{0.15}Mn_{1.75}O_4$ spinel oxides can also be formulated as $Li_{2.25}Mn_{4.18}O_9$ and $Li_{2.29}Ni_{0.33}Mn_{3.93}O_9$. We can consider these compounds to be defective spinels representative of the Li_2O-$yMnO_2$ system. The $LiMn_{1.86}O_4$ spinel possesses a unit cell parameter similar to that of the $Li_2Mn_4O_9$ system, where $a = 8.162$ Å [6]. The presence of nickel as a dopant in the spinel structure decreases the lattice parameter relative to $LiMn_{1.86}O_4$ as a result of the increased Mn^{4+} content and of the fact that the ionic radius of Ni^{2+} (0.74 Å) is smaller than that of Mn^{3+} (0.785 Å). The small value of the lattice parameter for the system doped with Fe can be explained by assuming that most tetrahedral sites are occupied by Fe^{3+}, and it can hence be ascribed to the small ionic radius of this ion in this environment (0.63 Å). The Al^{3+} ion is smaller than the Mn^{3+} ion in tetrahedral and octahedral coordination, and hence the unit cell dimension relative to the undoped spinel is decreased.

The number of vacancies in $LiMn_{1.86}O_4$ and $Li_{1.02}Ni_{0.15}Mn_{1.75}O_4$ spinel oxides is smaller than in the $Li_2Mn_4O_9$ structure. The lower oxygen-to-metal ratio [O/(Li + M + Mn) = 1.37] in the $Li_{1.02}Ni_{0.15}Mn_{1.75}O_4$ system can be ascribed to the presence of Ni^{2+} ions, which reduces the average oxidation state of metal ions (+3.67). The cation arrangement in the $LiMn_{1.86}O_4$ and $Li_{1.02}Ni_{0.15}Mn_{1.75}O_4$ phases may be similar to that in $Li_2Mn_4O_9$. The lithium ions must be located on A sites (the 8a crystallographic positions), the transition metal ions randomly distributed on B sites (the 16d crystallographic positions), and the oxygen ions at the 32e crystallographic positions. Based on the chemical analyses and on the above considerations, the defective spinels can be formulated according to the following cations distributions: $(Li)_{8a}(Mn_{1.86}\ \square_{0.14})_{16d}O_4$, $(Li)_{8a}(Li_{0.02}Ni_{0.15}\ Mn_{1.75}\ \square_{0.08})_{16d}O_4$, $(Li)_{8a}(Li_{0.03}Al_{0.15}Mn_{1.78}\ \square_{0.04})_{16d}O_4$ and $(Fe_{0.31}Li_{0.69})_{8a}(Li_{0.33}Mn_{1.75})_{16d}O_4$. In this last system, excess of Li^+ ions (0.08 atoms per formula) may be located in the remaining vacant positions (probably the 16c octahedral positions). Further justification of the location of Fe^{3+} and Ni^{2+} cations into the A and B sublattice, respectively, can be inferred from octahedral site preference energy, which reveals that tetrahedral site occupancy by Fe^{3+} and octahedral by Ni^{2+} is more favourable [11]. In contrast, it is more difficult to establish the Al^{3+} location with accuracy, though octahedral Al is found in many spinel oxides [12].

The spinels with a high Mn content exhibit abundant cation vacancies. This can be ascribed to the low synthesis temperature used (380 °C), which may be inadequate to obtain a stoichiometric spinel manganese oxide judging by the poor crystallinity reflected in the corresponding XRD patterns. Li-free Mn-Co spinels were found to behave similarly [10]. The defective $Li_2Mn_4O_9$ spinel oxide synthesized by Thackeray et al. [6, 9] at 380 °C is also poorly crystalline. This was confirmed by using the same carbonate, $Ni_{0.08}Mn_{0.92}CO_3$, to obtain spinel phases by heating at 550 and 800 °C. These last spinels, which preserve the same (M + Mn)/Li and M/Mn ratios, exhibit a loss of cation vacancies and a deficiency of oxygen atoms when the reaction temperature is raised (see Table 1).

Figure 2 shows the first galvanostatic cycle for Li-M-Mn-O-based electrodes (M = Al, Fe and Ni) recorded at a low current density (0.025 mA/cm^2). At this discharge rate, the Li-M-Mn-O spinels undergo insertion of slightly more than one Li^+ ion per formula unit to a cut-off voltage of 2.5 V. Based on a well-established reaction mechanism for lithium insertion into spinel oxides [13], this additional Li^+ ion must occupy the empty octahedral 16c sites. All four cells exhibit a well-defined step over this potential range reflecting as a voltage plateau at ca. 2.8 V. This is followed by a steep voltage decrease following insertion of an amount of lithium ions close to that required to achieve rock-salt stoichiometry. The major process in this step is expected to be the Mn^{4+}/Mn^{3+} reduction. The depth of discharge corresponding to the 2.8-V voltage plateau reduces the average oxida-

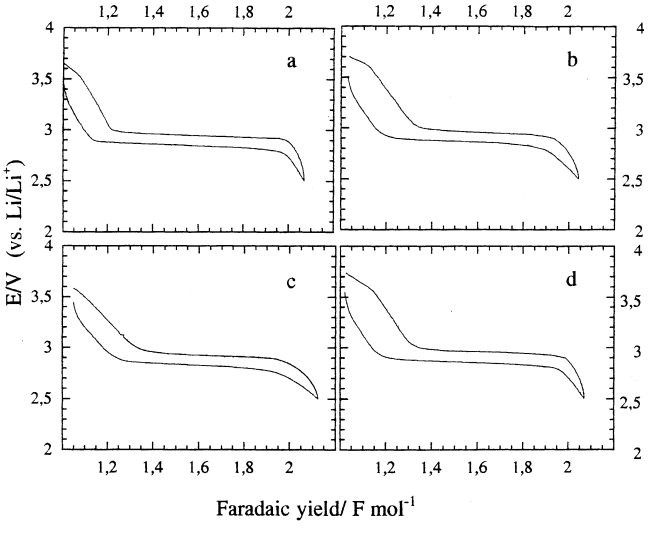

Fig. 2 Galvanostatic discharge-charge curve for Li/$LiClO_4$ (PC-EC)/Li-M-Mn-O oxide cells recorded at a 0.05 mA/cm^2 current density: **a** $LiMn_{1.86}O_4$, **b** $Li_{1.03}Al_{0.15}Mn_{1.78}O_4$, **c** $Li_{1.05}Fe_{0.31}Mn_{1.68}O_4$ and **d** $Li_{1.02}Ni_{0.15}Mn_{1.75}O_4$

tion state of manganese ions from 3.76 to 3.22 and from 3.67 to 3.27 for $LiMn_{1.86}O_4$ and $Li_{1.02}Ni_{0.15}Mn_{1.75}O_4$, respectively; these intervals are comparable to those for Li-Mn oxides with similar structures (e.g. for $Li_2Mn_4O_9$, where a change in Mn valence from 4.0 to 3.25 is needed to attain rock-salt stoichiometry). The average oxidation states of manganese ions obtained for the Li-Fe-Mn and Li-Al-Mn spinel systems after the first discharge plateau were 3.06 and 3.09, respectively. Also, the charge and discharge curves were rather close owing to the low average polarization of the electrode, which was about 100 mV in all four systems. The theoretical capacities calculated for these three spinel systems (Table 1) are lower than that for $Li_2Mn_4O_9$ (213 Ah/kg) but larger than that for the $LiMn_2O_4$ spinel phases (148 Ah/kg), except Li-Fe-Mn oxide, which has a similar theoretical capacity (142 Ah/kg).

Figure 3 shows the step potential electrochemical curves for Li/Li-M-Mn-O cells cycled between 4.4 V and 2.0 V, and further confirms the reversibility of the insertion-extraction process. The first cell discharge produces a single peak at 2.75 V corresponding to lithium insertion. In the charge process, four anodic peaks appear at 3.1 V, 3.75 V, 4.05 V and 4.20 V. The first peak corresponds to the removal of more than 75% of inserted lithium ions from the 16c octahedral sites. If one assumes the fulfilment of the model of Kock et al. [2], based on the remaining ions located in 8a positions migrating 16c sites simultaneously with the extraction, the voltage peaks at 4.05 and 4.20 V may correspond to lithium removal either from octahedral 16c sites or tetrahedral 8a sites. During the second discharge, the broad peak at 4.0 V corresponds to the reverse process for the anodic peaks at 4.05 V and 4.20 V, and can be ascribed to intercalation of the first lithium ion into λ-MnO_2, which occurs in different reaction steps.

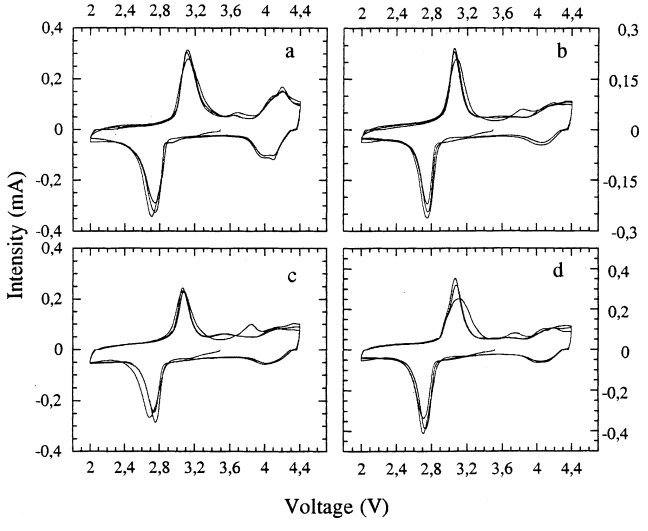

Fig. 3 Step potential electrochemical spectroscopy for lithium cells prepared from **a** $LiMn_{1.86}O_4$, **b** $Li_{1.03}Al_{0.15}Mn_{1.78}O_4$, **c** $Li_{1.05}Fe_{0.31}Mn_{1.68}O_4$ and **d** $Li_{1.02}Ni_{0.15}Mn_{1.75}O_4$

A singular peak is detected during cell charge at 3.75 V that was not observed in the cyclic voltammogram reported by Thackeray et al. [9] for the Li/$Li_2Mn_4O_9$ cell. On the other hand, a peak at similar voltage has been repeatedly reported in the literature for lithium insertion-extraction in various spinels such as $LiMn_2O_4$ [2, 9, 14] and $Li_{2.13}Co_{0.57}Mn_{3.66}O_9$ [10]. This peak has been ascribed to lithium extraction from octahedral sites as a result of manganese having an average oxidation state below +4 in the pristine oxide. This interpretation may also be extended to the Li-M-Mn-O phases studied in this paper (see Z_{Mn} in Table 1).

The considerably broadened peaks obtained in this work relative to the well-known typical voltammograms for Li/$LiMn_2O_4$ cells [2] may be attributed to the lower crystallinity of the Li-M-Mn-O spinel phases or to an overvoltage or impedance within the system.

Only one oxidation peak and a reduction peak were clearly observed around 3 V, suggestive of a reversible one-stage process by which a second lithium ion is inserted into the Li-M-Mn-O structures. We examined changes in the cycle performance of Li/Li-M-Mn-O cells between 3.3 and 2.3 V in the presence of various dopant metals (M = Al, Fe, Ni). Figure 4 shows the delivered cathode capacity for different cycles (calculated from the mass of spinel active material only, as the nominal formula shown in Table 1). There are some differences between the delivered cathode capacities for the first cycle and the theoretical capacities shown in Table 1 for the four spinel systems. The Li-Mn-O and Li-Al-Mn-O systems provide 155 and 157 Ah/kg, respectively, in the first discharge. These values correspond to a capacity loss of 12% and 9% relative to their respective theoretical values. These values are limited by the potential range (3.3 to 2.3 V) needed to ensure reversible conditions. By contrast, the Li-Ni-Mn and Li-Fe-Mn spinels exhibit different behaviour over the same cycling voltage range. The delivered cathode capacity for the first cycle was 170 and 160 Ah/kg for the Li-Ni-Mn and Li-Fe-Mn

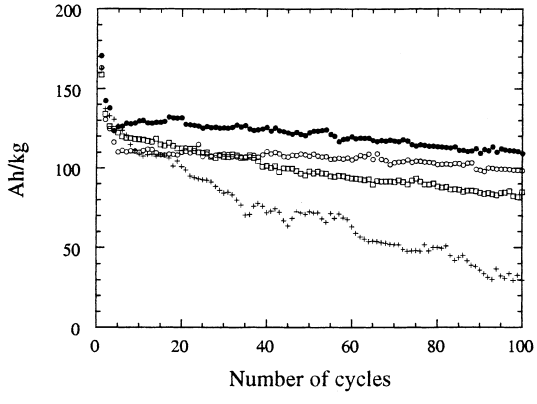

Fig. 4 Delivered cathode capacity from galvanostatic cycling of Li/$LiClO_4$(PC-EC)/Li-M-Mn-O cells at a 0.25 mA/cm^2 current density: $LiMn_{1.86}O_4$ (□), $Li_{1.03}Al_{0.15}Mn_{1.78}O_4$ (+), $Li_{1.05}Fe_{0.31}Mn_{1.68}O_4$ (○) and $Li_{1.02}Ni_{0.15}Mn_{1.75}O_4$ (●)

oxides, respectively, and hence 3% and 12% higher than their respective theoretical capacities. For Fe, this behaviour is rather surprising taking into account the low average valence of Mn and the occupancy of some 16c positions. It may be to the presence of other manganese phases with a similar electrochemical behaviour in the cathode material. Unfortunately, the poor crystallinity of these compounds makes it difficult to discern different phases in the XRD pattern with adequate accuracy.

The $Li_{1.03}Al_{0.15}Mn_{1.78}O_4$ and $LiMn_{1.86}O_4$ oxides exhibited a sustained capacity loss as the number of cycles was increased; the loss was more pronounced for the Al-doped spinel. In any case, these cation-deficient spinels obtained from a carbonate precursor exhibit a better cycling performance than other, similar spinels used as cathodes in 3-V lithium cells [15]. The Li/Li-Ni-Mn and Li/Li-Fe-Mn cells were found to exhibit better cycling performance. While the initial capacity in these systems decreases abruptly during the first five cycles, it soon levels off at 120 and 105 Ah/kg for the Ni-Mn and Fe-Mn cells, respectively. These values are preserved almost unaltered over the next 100 cycles. After 200 cycles, both systems retain about 80% of their initial cell capacity. This is especially advantageous taking into account that these cells are built from Li metal as anode and the surface of this metal is known to be difficult to reconstruct after several cycles, thus shortening the cycle life of the cell.

Also, these two systems are superior in electrochemical performance to $Li_{2.13}Co_{0.57}Mn_{3.66}O_9$, a cathodic material for 3.0-V lithium cells recently studied by our research group [10]. This is especially outstanding for the Li-Ni-Mn phase, which exhibits an increased capacity during the first 100 cycles (115 Ah/kg vs 104 Ah/kg). Besides these advantages, Ni and Fe are more inexpensive and less toxic than Co.

As yet, there is no plausible explanation for the relationship between the metal dopant and capacity changes during cycling. The limited cyclability of $LiMn_2O_4$ used as the cathode in 3-V Li cells has been associated with the cubic-to-tetragonal phase transition induced by a Jahn-Teller effect [6]. This assumption can be extended to the $LiMn_{1.86}O_4$ phase, even though the poor crystallinity of this solid makes it difficult to confirm the formation of a tetragonal phase such as that observed in well-crystallized $Li_{1+x}AlMnO_4$ systems upon lithium insertion [15]. It is unclear whether the improved cycling performance is a result of the mitigation of the Jahn-Teller effect caused by the dopant metal (at least for Al). Attempts at inserting other non-transition metals such as Mg failed. Ca gave a carbonate solid solution, but the fired sample was found to contain not only the spinel compound but also unresolved phases. In any case, the electrochemical behaviour was similar to that of Al. The results suggest that, when the dopant is a transition metal, it has a favourable effect on the structural flexibility of the spinel, irrespective of the lattice site to be occupied. Probably, this favourable effect is consequence of the *d* electrons in the metal. These findings agree well with the results of computer simulation studies performed by Shigematsu et al. [16] assessing the energy change associated with the structural change in $LiMe_{0.5}Mn_{1.5}O_4 \Leftrightarrow Li_2Me_{0.5}Mn_{1.5}O_4$ (Me = transition metal). Based on these calculations, elements such as Fe, Co, Ni are expected to suppress the structural change.

With the aim of improving the electrochemical performance of the Li-Ni-Mn system, we prepared this spinel at two higher temperatures, viz. 550 and 800 °C in air for 20 h. The XRD patterns shown in Fig. 5 correspond to a cubic spinel structure and, as expected, reveal a substantial decrease in peak width with the increasing firing temperature that results in increased crystallinity. Lattice parameters and composition data are included in Table 1. Increasing the heating temperature decreases the average Mn oxidation through oxygen loss from the spinel structure. This oxygen release was also confirmed by the thermogravimetric curve for the sample prepared at 380 °C. The increase in Mn^{3+} was also reflected in a simultaneous increase in the unit cell dimension. Scanning electron micrographs (Fig. 6) provide valuable information on particle morphology and its changes with temperature. The low-temperature sample was found to consist of conglomerates that were

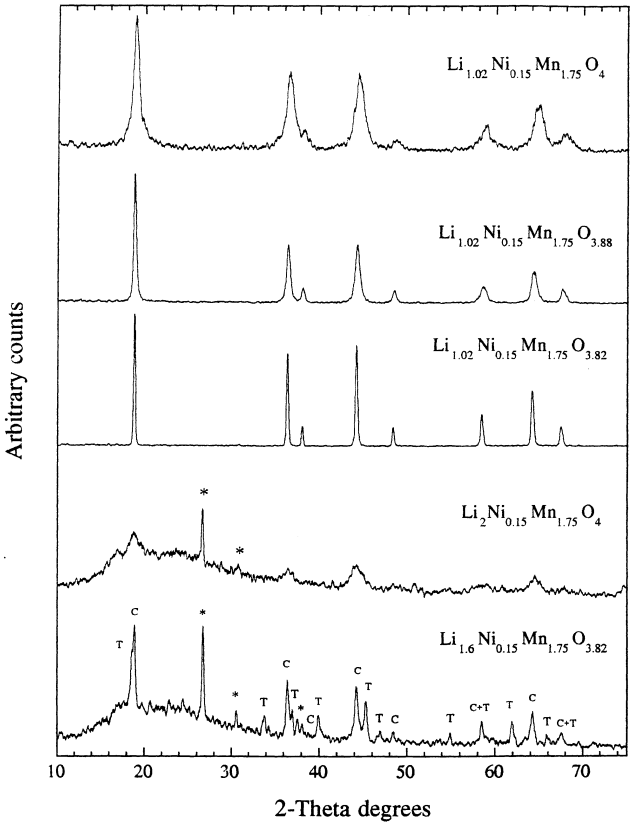

Fig. 5 Powder X-ray diffraction patterns for Li-Ni-Mn-O oxides synthesized at different temperatures and for their lithiated products showing, graphite reflections (∗), tetragonal spinel phase reflections (T), and cubic spinel phase reflections (C)

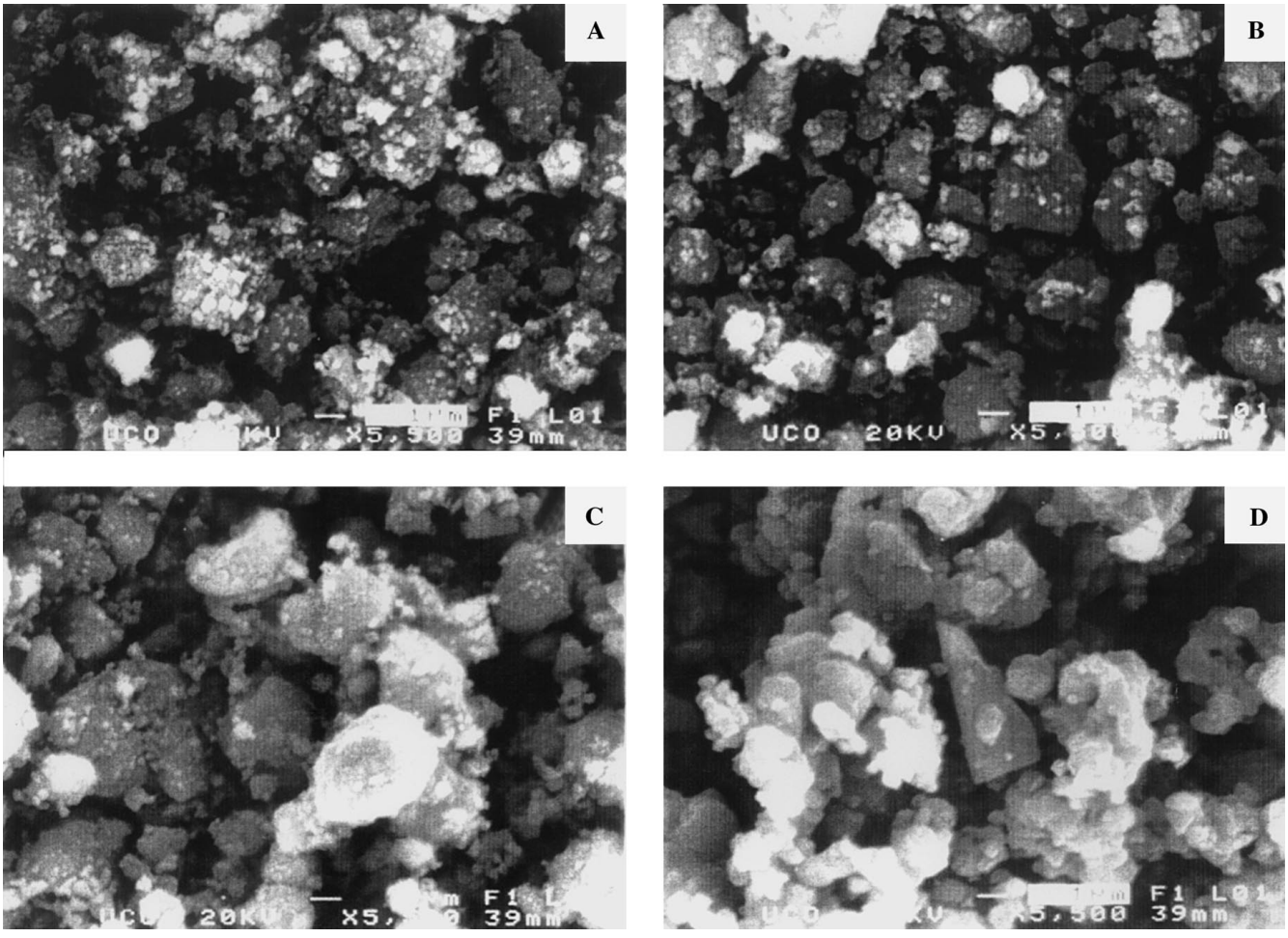

Fig. 6 Scanning electron micrographs for spinel oxide particles: **A** $LiMn_{1.86}O_4$ [380 °C], **B** $Li_{1.02}Ni_{0.15}Mn_{1.75}O_4$ [380 °C], **C** $Li_{1.02}Ni_{0.15}Mn_{1.75}O_{3.88}$ [550 °C] and **D** $Li_{1.02}Ni_{0.15}Mn_{1.75}O_{3.82}$ [800 °C]

rotund in shape and uniform in size (about 1–2 μm). On their surface lay smaller particles with a marked tendency to agglomerate. Increasing the synthesis temperature caused the rotund particles to adopt polygonal shapes and the smaller particles to sinter and disappear.

For comparison, Fig. 7 shows the delivered capacity of the three Li/Li-Ni-Mn-O cells as a function of the number of cycles. As can clearly be seen, the main conclusion one can draw from this plot is that there is a deterioration of the cycling performance on increasing the firing temperature. Changes in particle morphology can be discarded as the cause. In fact, the $LiMn_{1.86}O_4$ solid and the different Ni doped spinels exhibit particles of similar shape (Fig. 6) despite their different electrochemical cycling behaviour. The cause must be related to structural changes in the spinel induced by the lithium insertion process. Figure 5 shows the XRD patterns for partially lithiated phases in low- and high-temperature samples. The latter exhibit new reflections and their difractogram can be indexed on a tetragonal system with unit cell parameters $a = 8.04(1)$ Å and $c = 8.99(1)$ Å. Thus, one can assume the change in crystal symmetry

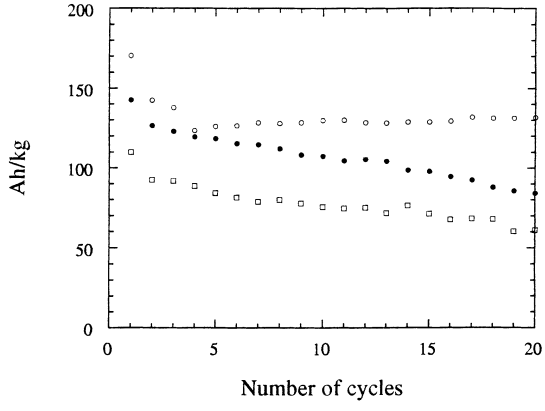

Fig. 7 Delivered cathode capacity from galvanostatic cycling of $Li/LiClO_4$(PC-EC)/Li-Ni-Mn-O cells at 0.25 mA/cm^2 current density: $Li_{1.02}Ni_{0.15}Mn_{1.75}O_4$ (○), $Li_{1.02}Ni_{0.15}Mn_{1.75}O_{3.88}$ (●) and $Li_{1.02}$-$Ni_{0.15}Mn_{1.75}O_{3.82}$ (□)

caused by the Jahn-Teller effect to be responsible for the impaired electrochemical performance. By contrast, the low-temperature spinel maintains cubic symmetry during the lithium insertion process. This means that avoiding Jahn-Teller distortion entails not only using an appropriate dopant metal ion but also starting from a highly disordered structure.

Conclusions

New spinel phases of formulae $LiMn_{1.86}O_4$, $Li_{1.03}Al_{0.15}Mn_{1.78}O_4$, $Li_{1.05}Fe_{0.31}Mn_{1.68}O_4$ and $Li_{1.02}Ni_{0.15}Mn_{1.75}O_4$ were obtained at low temperatures, using mixed carbonates as precursors. These oxides improve on the cycle life of similar rechargeable 3-V Li/Li-M-Mn-O cells at room temperature. Specially good is the electrochemical performance of $Li/Li_{1.05}Fe_{0.31}Mn_{1.68}O_4$ and $Li/Li_{1.02}Ni_{0.15}Mn_{1.75}O_4$ cells cycled between 3.3 and 2.3 V. The highly disordered structure of these systems significantly lessens Jahn-Teller distortion. In fact, if the spinel crystallinity is improved by raising the synthesis temperature, the capacity fades rapidly on cycling as a result. In these high-temperature spinels, the occurrence of a Jahn-Teller effect is apparent from the cubic-to-tetragonal phase transition caused by lithium insertion. Such as a phase transition is undetectable in the low-temperature samples. From these preliminary results, the $Li_{1.02}Ni_{0.15}Mn_{1.75}O_4$ spinel can be regarded as a promising cathode material for rechargeable lithium batteries.

Acknowledgements This work was supported by Spain's Ministerio de Educación y Cultura (CICYT Project PB95-0561) and the Junta de Andalucía (Group FQM-175).

References

1. Ohzuku T, Kitagawa M, Hirai T (1989) J Electrochem Soc 136: 3169
2. Rossouw MH, de Kock A, de Picciotto LA, Thackeray MM, David WYF, Ibberson RM (1990) Mater Res Bull 25: 173
3. Barboux P, Tarascon JM, Shokoohi FK (1991) Solid State Chem 94: 185
4. Tarascon JM, Wang E, Shokoohi FK, McKinnon WR, Colson S (1991) J Electrochem Soc 138: 2859
5. Manev V, Momchilov A, Nassalevska A, Kozawa A (1993) J Power Sources 41: 305
6. Thackeray MM, de Kock A, Rossouw MH, Liles D, Bittihn R, Hoge D (1992) J Electrochem Soc 139: 363
7. Huang H, Bruce PG (1994) J Electrochem Soc 141: L76
8. Amine K, Tukamoto H, Yasuda H, Fujita Y (1996) J Electrochem Soc 143: 1607
9. Thackeray MM, de Kock A, David WYF (1993) Mater Res Bull 28: 1041
10. Sánchez L, Tirado JL (1997) J Electrochem Soc 144: 1939
11. Pistoia G, Antonini A, Rosati R, Bellitto C, Ingo GM (1997) Chem Mater 9: 1443
12. Huheey JE (1978) Inorganic Chemistry. Harper and Row, p 373
13. Thackeray MM, David WYF, Bruce PG, Goodenough JB (1983) Mater Res Bull 18: 461
14. Siury H, Schlörb H, Rahner D, Plieth W (1996) International Meeting on Lithium Batteries, Nagoya, Japan. Electrochemical Society of Japan, p 466
15. Le Cras F, Bloch D, Anne M, Strobel P (1996) Solid State Ionics 89: 203
16. Usami K, Saito H, Shigematsu K (1996) International Meeting on Lithium Batteries. Nagoya, Japan. Electrochemical Society of Japan, p 480